Published in final edited form as:
J Neurosci Res. 2010 November 1; 88(14): 3206–3214. doi:10.1002/jnr.22470.

Cerebral tissue repair and atrophy after embolic stroke in rat: an MRI study of Erythropoietin therapy

Guangliang Ding, PhD[1], **Quan Jiang, PhD**[1], **Lian Li, PhD**[1], **Li Zhang, MD**[1], **Ying Wang, MD**[1], **Zheng Gang Zhang, PhD & MD**[1], **Mei Lu, PhD**[2], **Swayamprava Panda, MS**[1], **Qingjiang Li, MBA**[1], **James R. Ewing, PhD**[1], and **Michael Chopp, PhD**[1,3]

[1]Department of Neurology, Henry Ford Hospital, 2799 West Grand Boulevard, Detroit, MI 48202, USA.

[2]Department of Biostatistics and Research Epidemiology, Henry Ford Hospital, 2799 West Grand Boulevard, Detroit, MI 48202, USA.

[3]Department of Physics, Oakland University, Rochester, MI 48309, USA.

Abstract

Using magnetic resonance imaging (MRI) protocols of T_2-, T_2*-, diffusion- and susceptibility-weighted imaging (T2WI, T2*WI, DWI and SWI) with a 7T system, we tested the hypothesis that treatment of embolic stroke with Erythropoietin (EPO) initiated at 24 hours and administered daily for 7 days after stroke onset has benefit on repairing ischemic cerebral tissue. Adult Wistar rats were subjected to embolic stroke by means of middle cerebral artery occlusion (MCAO) and were randomly assigned to a treatment (n=11) or a control group (n=11). The treated group was given EPO intraperitoneally at a dose of 5,000 IU/kg daily for 7 days starting 24h after MCAO. Controls were given an equal volume of saline. MRI was performed at 24h and then weekly for 6 weeks. MRI and histological measurements were compared between groups. Serial T2WI images demonstrated that expansion of the ipsilateral ventricle was significantly reduced in the EPO treated rats. The volume ratio of ipsilateral parenchymal tissue relative to the contralateral hemisphere was significantly increased after EPO treatment compared with control animals, indicating that EPO significantly reduces atrophy of the ipsilateral hemisphere, although no significant differences in ischemic lesion volume were observed between the two groups. Angiogenesis and white matter remodeling were significantly increased and occurred earlier in EPO treated animals than in the controls, as evident from T2*WI and diffusion anisotropy maps, respectively. These data indicate that EPO treatment initiated 24h post stroke promotes angiogenesis and axonal remodeling in the ischemic boundary, which may potentially reduce atrophy of the ipsilateral hemisphere.

Keywords

brain atrophy; cerebral tissue repair; erythropoietin; embolic stroke; magnetic resonance imaging

Introduction

The majority of ischemic stroke patients do not receive thrombolytic treatment with intravenous injection of tissue-type plasminogen activator (tPA), due to the short therapeutic

Please send all correspondence to: Michael Chopp, Ph.D., Henry Ford Hospital, Neurology Department, E&R 3056, 2799 West Grand Boulevard, Detroit, MI 48202, Tel: 313-916-3936, Fax: 313-916-1318, chopp@neuro.hfh.edu.

Conflict of interest disclosures None.

window after onset of ischemia (Grotta et al, 2001; Morgenstern et al, 2002). Clinical trials of neuroprotective treatments for acute stroke patients have failed (Adams et al, 2003, 2005; Ovbiagele et al, 2003). Thus, cerebral tissue reparative therapy warrants development for the treatment of ischemic stroke.

Endogenous reparative processes of cerebral tissue, including angiogenesis and neurogenesis, are initiated after stroke onset (Krupinski et al, 1994; Plate et al, 1999; Cramer & Chopp, 2000; Zhang et al, 2000; Parent et al, 2002; Yu et al, 2007). Focal ischemic injury increases neurogenesis in the subventricular zone, directs neuroblast migration to sites of damage, and neuroblasts are capable of replacing some neurons lost after ischemic injury (Parent et al, 2002; Zhang et al, 2001, 2004). However, few newborn cells survive long-term to become functional striatal neurons (Arvidsson et al, 2002; Parent et al, 2002). Angiogenesis couples to neurogenesis (Ohab et al, 2006; Teng et al, 2008) and creates a microenvironment that supports the migrating neuroblasts to survive and integrate into the parenchymal tissue (Plane et al, 2008). Thus, a strategy to enhance endogenous cerebral tissue repair likely will include treatments which augment neurogenesis and angiogenesis and promote the mutual interaction between neurogenesis and angiogenesis (Parent and Silverstein, 2007, Zhang and Chopp, 2009).

Erythropoietin (EPO) is a hematopoietic cytokine (Jelkmann and Hellwig-Burgel, 2001). EPO reduces neuronal apoptosis (Ghezzi and Brines, 2004; Siren et al, 2006), and the therapeutic profile of EPO is complex with anti-apoptotic, anti-oxidant, anti-inflammatory and neurotrophic properties (Siren et al, 2006). Delayed EPO treatment of embolic stroke in rats at a dose of 5,000 IU/kg administered intraperitoneally starting at 24 hours and continuing daily for 7 days after middle cerebral artery (MCA) occlusion (MCAO) augmented angiogenesis, neurogenesis, white matter plasticity, and increased cerebral vascular endothelial growth factor (VEGF) and brain-derived neurotrophic factor (BDNF) expression, with no effect on infarct volume (Wang et al, 2004; Li et al, 2009). These effects of delayed EPO treatment may repair cerebral tissue and resist brain atrophy after stroke in rat.

In the present study, we employed magnetic resonance imaging (MRI) methods to monitor cerebral responses (Ding et al, 2008a; 2008b; Li et al, 2007) to the delayed EPO treatment of stroke. We investigated the therapeutic benefit of the delayed EPO treatment in rats with embolic stroke, particularly its capacity to protect cerebral tissue against brain atrophy.

Materials and Methods

Animals and Experimental Protocol

All studies were performed in accordance with institutional guidelines for animal research and approved by the IACUC of Henry Ford Hospital.

Adult male Wistar rats (Jackson Laboratory, Bar Harbor, ME) 8–12 weeks of age and weighing 300 to 350 g were subjected to embolic stroke. This model of embolic stroke provides a reproducible infarct volume localized to the territory supplied by the MCA (Zhang et al., 1997). Briefly, an aged white clot (blood of a rat was withdrawn into 20cm PE-50 tubing), which was prepared 24 hours (retained at 25°C for 2h and at 4°C for 22h) before ischemia, was slowly injected into the internal carotid artery to the origin of the MCA. The stroke rats were randomly assigned to either the treatment (n = 11) or control group (n = 11).

In the treatment group, recombinant human EPO (epoetin α AMGEN) was administered intraperitoneally at a dose of 5,000 IU/kg daily for 7 days starting 24 hours after MCAO.

This dose (5,000 IU/kg) and treatment protocol has been shown to enhance neurorestorative and neuronal improvements after stroke in the embolic MCAO model (Wang et al, 2004). The control group received an equal volume of saline.

MRI and functional tests were performed before stroke and at 24h and weekly to 6 weeks after stroke for all rats. All animals were euthanized 6 weeks after stroke. Functional tests, MRI and histological data analyses were performed in a double blind fashion.

MRI Measurements

MRI was performed using a 7 Tesla Bruker system (Bruker-Biospin, Billerica, MA). MRI scan before stroke was performed to exclude abnormal rats. MRI images after stroke were obtained at 24 hours, then once a week for 6 weeks. A radio-frequency (RF) saddle coil was used as the transmitter and an actively RF decoupled surface coil as the receiver. Stereotaxic ear bars were attached to minimize movement, and anesthesia was maintained using a mixture of nitrous oxide (70%), oxygen (30%), and halothane (0.75–1.00%). Rectal temperature was kept at 37 ± 1.0 °C using a feedback controlled water bath. A tri-pilot imaging sequence was used to ensure reproducible positioning of the animal in the magnet at each MRI session.

T_2-weighted imaging (T2WI) were performed taking multiple slices (13 slices, 1 mm slice thickness) and using a multiple spin with a 32×32 mm^2 field-of-view (FOV) and a 128×64 image matrix. All six echoes were acquired with an equal interval echo time (TE). The TE was 15 ms. Repetition time (TR) was 8 seconds. The sequence took about 9 minutes.

T_2*-weighted imaging (T2*WI) were performed with multiple slices (13 slices, 1 mm slice thickness) and using a multiple gradient echo sequence, with a 32×32 mm^2 FOV and a 128×64 image matrix. All six echoes were acquired with an equal interval TE of 3.6 ms and the same read-out gradient polarity. The TR was 8 seconds. The sequence took about 9 minutes.

Susceptibility weighted imaging (SWI) (Haacke et al, 2004) employed a 3D gradient echo imaging sequence with calculated gradient trims to comprise the first-order flow compensation achieved via gradient-moment nulling in all three directions of read, phase and slice. The acquisition matrix was set as 256×256×96 for fitting the field-of-view (FOV) 32×32×24mm^3. TR and TE were 50ms and 10ms, respectively. The 500μs Gaussian RF pulse generated a flip angle of approximately 15 degrees.

Arterial spin labeling (ASL) was used to quantify cerebral blood flow (CBF) in cerebral tissue. The adiabatic inversion pulse was a continuous RF power wave of approximately 0.3 kHz at a frequency offset of 6 kHz and accompanied an axial gradient of 0.3 kHz/mm. A spin echo imaging sequence with TR/TE = 1000 ms/20 ms was followed. The imaging slice was 1 mm thick and 2 cm distal from the labeled slice. An image average was applied by reversing the gradient polarities. FOV was 32×32 mm^2, matrix 64×64 and scan time 18 minutes.

Diffusion-weighted imaging (DWI) was performed with three b-values of 20, 600 and 1200 s/mm^2 at three orthogonal directions along the X, Y and Z axes. Two 10 ms (δ) gradient pulses separated by 18 ms (Δ) on either side of the refocusing RF pulse were in spin echo sequence with a 32×32mm^2 FOV, 128×64 matrix, 13 slices and 1 mm slice thickness. TR was 1500 ms and TE was 40 ms.

Histology

To examine the cerebral microvessels, 1 ml fluorescein isothiocyanate (FITC) dextran (2×10^6 Daltons, Sigma, St. Louis, MO; 50mg/ml) was administered intravenously 5 minutes before sacrifice. Animals were anesthetized with ketamine (44mg/kg i.p.) and xylazine (13mg/kg i.p.) and transcardially perfused with heparinized saline followed by 10% neutral buffered formalin. The brain was immersed in 4% paraformaldehyde in phosphate buffered saline at 4 °C overnight, and the next morning seven 2mm-thick blocks of brain tissue were cut, processed and embedded in paraffin.

The MicroComputer Imaging Device (MCID) system (Imaging Research, Ontario, Canada) and the MRC 1024 laser scanning confocal microscopy (LSCM) (Bio-Rad, Cambridge, MA) were used for histological measurements. Coronal sections were cut from each block. Sections of 6 μm thick were stained with hematoxylin and eosin (H&E) to evaluate cerebral infarction or with double Bielschowsky's silver (modified) and Luxol fast blue (B&LFB) to evaluate myelinated axons (Wakefield et al, 1994), by using the MCID system with a 40× objective (Olympus BX40) and a 3-CCD color video camera (Sony DXC-970MD). Sections of 100 μm thick were perfused with FITC-dextran to examine the cerebral microvasculature by LSCM. Four FOVs in each coronal section were used for quantification. The immunoreactive areas at each site (as a percentage of the field-of-view) were measured under an optical microscope using the 40× objective at the boundary of the ischemic lesion and the homologous contralateral region and the data digitized to assess axonal density using an average of two FOVs for each location.

Data analysis and statistics

The MRI images were analyzed with a homemade Eigentool software package in Sun workstations (Peck et al, 1992). All two-dimensional (T2WI, T2*WI, CBF and DWI) images were reconstructed using a 128×128 matrix. T_2 or T_2* maps were produced using linear least-squares fit to the plot of the natural logarithm of T2WI or T2*WI image intensities versus TE values. Apparent diffusion coefficient of water (ADC_w) map was produced using linear least-squares fit to the plot of the natural logarithm of DWI image intensities versus b-values. Diffusion anisotropy (DA) map was derived from three ADC_w maps along X, Y and Z directions using the following formula (van Gelderen et al, 1994):

$$DA = \sqrt{\frac{1}{6}} \frac{\sqrt{(D_x - D_{av})^2 + (D_y - D_{av})^2 + (D_z - D_{av})^2}}{D_{av}} \quad (1)$$

where $D_{av} = (D_x + D_y + D_z)/3$.

The tissue parametric maps and histological images were co-registered (Jacobs et al, 1999) and analyzed using the Eigentool package. T2WI images are referred to as reference images in co-registration and warping. Ventricular and ischemic lesion size were determined by T_2 maps acquired after stroke, using values above the mean plus two standard deviations (SD) of the contralateral measurements (Hoehn-Berlage et al, 1995; Ding et al, 2004). The total volume of the lateral ventricle was the sum of the volumes in the five central slices that included major volume of lateral ventricle and ischemic lesion (Fig. 1). Hemispheric volumes were measured using the same five slices. In a few cases, ischemic lesion areas were not distinguished from ventricle on T_2 maps, as shown in Fig. 2 a. Various MRI images, e.g. an SWI image acquired post gadolinium-diethylenetriamine penta-acetic acid (Gd-DTPA) injection into the rat tail vein (Fig. 2 b), were used in such situations to find the boundary of the ventricle, as indicated by red arrows in Fig. 2 b, to separate the ventricle and lesion. In these cases, 2D axial images extracted from SWI were downsized to 128×128 and

registered to T_2 maps. The border of ventricle was identified as a ROI on these SWI images, and the ROI was copied onto T_2 map for measurement.

The CBF map (f-value) was calculated according to equation:

$$f = \frac{\lambda}{T_{1app}} \frac{[M^{cont} - M^{inv}]}{2M^{cont}} \quad (2)$$

where λ is blood/brain partition coefficient for water, T_{1app} is apparent T_1 relaxation time of brain water in the absence of flow or exchange between blood and brain. M^{cont} and M^{inv} are the control and inversion image intensities, respectively. A value of 0.9 g/mL for λ and 1.7 seconds for T_{1app} were used for CBF calculation (Williams et al, 1992).

MRI observations and histological measurements are summarized as mean ± SD. Differences in the MRI or histological data between groups were analyzed by a mixed model of analysis of variance (ANOVA) and covariance (ANCOVA), or two-tailed *t*-test, respectively. The significance level (α) was set at 5%. For the longitudinal MRI measurements, the analysis started testing the group and time (without baseline time point) interaction, followed by testing the group difference at each time point if the interaction or overall group effect was detected at the 0.05 level.

Results

The ischemic lesion volumes 6 weeks after stroke measured on T_2 maps were 38.6 ± 12.8 percent of the ipsilateral hemispheric volume for EPO treated rats and 31.8 ± 12.0 percent for the controls. No significant differences were observed between the two groups ($p > 0.2$).

T_2 maps obtained 6 weeks after stroke from an EPO-treated rat (Fig. 2 c) and a control rat (Fig. 2 d), with approximately the same size of stroke lesion identified by T_2 thresholds as indicated by red borders in Fig. 2 c & d, visually demonstrated that the ipsilateral ventricle expansion was diminished in the EPO treated rat compared to the control one. The serial T_2-relaxation maps of a representative EPO treated rat exhibited gradual expansion of the ipsilateral ventricle starting 1 to 6 weeks after stroke compared to the contralateral ventricle (Fig. 3, the upper row). In contrast, the ipsilateral ventricular volume in a representative control rat (Fig. 3, the lower row) exhibited both faster and greater expansion than the EPO treated animals. H&E sections (Fig. 3, the last column) histologically confirmed the MRI findings. The ipsilateral ventricle was smaller than the contralateral ventricle at 24 hours after stroke (Fig. 3, the first column), with mean values of 14.4±3.3mm^3 *vs* 16.1±4.3mm^3 measured in T_2 maps overall the rats, likely, because it was compressed by the edema in the swollen cerebral tissue.

Quantitative data demonstrated that, in all animals, ventricular volume in the ipsilateral hemisphere increased from 1 week to 6 weeks after stroke. However, this expansion was reduced in EPO treated animals compared to control animals. Increases of ventricular volume in the ipsilateral hemisphere were examined in terms of the volume ratios (ipsilateral *vs* contralateral) for both treated and control groups (Fig. 4). Using the T2WI measurements, ventricular volume ratios of both treated and control groups increased monotonically from 1 to 6 weeks after stroke; however, the mean ratio was significantly lower in the EPO treated group starting 4 weeks after stroke than in the control group (Fig. 4 a). The mean ratio 6 weeks after stroke was 1.99 ± 0.22 for the treated rats ($n = 11$) and 2.34 ± 0.33 for the controls ($n = 11$), a significant difference ($p < 0.01$).

Measurements of cerebral hemisphere volume using T2WI images demonstrated atrophy of rat brain after stroke (Fig. 4 b). In all animals by 24 hours after stroke, the ipsilateral hemisphere was swollen due to edema and was larger than the contralateral hemisphere. The average hemispheric volume ratio (ipsilateral *vs* contralateral) approached 1.0 by 1 week after stroke, but it decreased once the edema dissipated. For the treated rats, the mean volume ratios reached the lowest values (0.940 ± 0.038) 4 weeks after stroke, while for the controls, the lowest volume ratio was 0.913 ± 0.036 at 5 weeks after stroke. These volume ratios were significantly different between groups at 5 and 6 weeks after stroke ($p < 0.05$ and 0.02, respectively).

Considering both expansion of the ventricle and atrophy of the ipsilateral hemisphere, decreases in parenchymal volume (excluding the ventricle from the hemisphere) were examined as ratios of parenchymal volume (ipsilateral *vs* contralateral). Changes in parenchymal ratio were similar to hemispheric ratio since the lateral ventricle accounts for a minor part of the hemispheric volume (Fig. 4 c). Cerebral tissue loss (*i.e.* the decrease of parenchymal volume) in the EPO treated rats was significantly reduced at 5 and 6 weeks after stroke compared with the controls ($p < 0.05$ and 0.02, respectively).

The ANCOVA exhibited that the probability factor of overall effect of group by time were $p < 0.03$ for ventricle, $p < 0.002$ for hemisphere and $p < 0.003$ for parenchymal between treated and control animals, which indicated that treatment effects were depended on the time.

As a baseline, we measured the volumes of the contralateral ventricle and hemisphere for all animals with T_2-relaxation maps. The data are listed in Table 1. At 24h after stroke, the contralateral cerebral tissue was compressed by the ipsilateral swollen cerebral tissue because of edema after ischemia. Thus, the contralateral hemispheric volume was smaller than its volume measured at other time points. No significant differences were observed at 6 weeks after stroke in the volume of the contralateral hemisphere between EPO-treated and control rats ($p > 0.9$). Moreover, the differences of hemispheric volumes between 1 week and 6 weeks after stroke, by applying paired t-test, were not significant for both groups (EPO: $p > 0.7$ & saline: $p > 0.7$). T2WI measurements of the ventricle volume exhibited the same results as the hemispheric volume. No significant differences were observed at 6 weeks after stroke between the two groups ($p > 0.1$), or between 24h and 6 weeks after stroke for EPO-treated ($p > 0.4$) and saline-treated ($p > 0.1$) animals, respectively.

In EPO-treated rats, angiogenesis is typically detectable starting 2 weeks after stroke by T_2* map (Fig. 5 a) or SWI (Fig. 5 b). Histological images of FITC-dextran stained sections showed increased intensity with hyperdense microvessels in this region (Fig. 5 c), confirming the enhanced angiogenesis. Likewise, elevated CBF resulting from the enhanced angiogenesis was evident by 4 weeks on the CBF map (Fig. 5 d, red arrow). However, in the controls, angiogenesis is not detectable until 4 weeks after onset of stroke by T_2* map (Fig. 5 g) or SWI (Fig. 5 h). FITC-dextran stained sections along the ischemic boundary revealed more extensive microvessels in the EPO-treated rats (Fig. 5 c) than in the controls (Fig. 5 i). Microvascular density measured by LSCM was significantly ($p < 0.05$) increased in the EPO-treated group (597.4 ± 81.9 vessels/mm^2) compared with the control group (496.2 ± 83.3).

Diffusion anisotropy, an indicator of enhanced white matter plasticity, gave similar results. By 4 weeks after stroke, increased DA values (Fig. 5 e, red arrow), representing increased white matter reorganization (*i.e.*, density and orientation), was detected in the same area as the increased angiogenesis (Fig. 5 a) and elevated CBF (Fig. 5 d) in the representative EPO treated rat. The Bielschowsky's silver and Luxol fast blue stained sections demonstrated

increased numbers of axons and highly ordered neuronal fibers in this region (Fig. 5 f). Ratios of fiber density, compared to the homogeneous tissue in the contralateral hemisphere, were 1.40 ± 0.23 for the EPO treated group and 1.16 ± 0.12 for the controls in the FOV along the ischemic boundary. The differences were significant ($p < 0.03$).

Neurological function tests demonstrated that the modified neurological severity score (mNSS) was significantly improved in EPO-treated animals ($n = 11$) compared to controls ($n = 11$) at 5 weeks (4.5 vs 5.9, $p < 0.03$) and 6 weeks (5.0 vs 6.3, $p < 0.04$) after stroke.

Discussion

The present study shows that treatment of embolic stroke in rats with 5,000 IU/kg EPO administered intraperitoneally starting 24 hours after MCAO and continuing daily for 7 days not only augments angiogenesis and white matter reorganization, but also protects brain tissue from further loss, leading reductions in expansion of the ipsilateral ventricle and shrinkage of the ipsilateral hemisphere, though the delayed treatment of EPO does not decrease infarct volume.

Angiogenesis and neurogenesis are evoked soon after stroke (Krupinski et al, 1994; Plate et al, 1999; Cramer & Chopp, 2000; Zhang et al, 2000; Parent et al, 2002; Yu et al, 2007), and angiogenesis also mutually interacts with neurogenesis (Ohab et al, 2006; Teng et al, 2008). Angiogenic vessels release neurotrophic factors, such as BDNF, into their microenvironment. Neurogenesis increases in the adult forebrain subventricular zone after stroke. Newborn neurons migrate to the peri-infarct striatum after stroke (Zhang et al, 2005; Plane et al, 2008). The delayed EPO treatment enhances angiogenesis and neurogenesis after stroke by increasing VEGF and BDNF (Wang et al, 2004). Thus, the delayed EPO treatment may facilitate ischemic tissue repair by improving the ischemic boundary microenvironment to reduce death of resident brain cells and increase survival of neuroblasts migrating from the subventricular zone. In concert, all of these events may lead to reduction in the brain atrophy after stroke.

Our MRI and histological measurements in the present study demonstrate the temporal profile of the cerebral repair process. Increased angiogenesis in the delayed EPO treated rats was evident 2 ~ 3 weeks after stroke by T_2* map or SWI (Fig. 5 a, b). Newly-formed vessels in the ischemic boundary regions appear to be functional, based on elevation of local cerebral blood flow in the same region, observed 2 weeks after the MRI identified angiogenesis (Fig. 5 d), and as confirmed by histological analysis of FITC-dextran stained sections (Fig. 5 c). Thus, along the ischemic boundary, simultaneously enhanced angiogenesis and neurogenesis induced by EPO (Wang et al, 2004) mutually interacted and coupled via VEGF (Teng et al, 2008) to improve survival and integration of newborn neurons into neuronal system, which may lead white matter outgrowth and reorientation (*i.e.* reorganization). Reorganized neuronal fibers were detected at 4 weeks after stroke in this study by MRI DA map (Fig. 5 e), which was confirmed histologically by Bielschowsky's silver and Luxol fast blue staining (Fig. 5 f). The neurological function score was significantly improved starting 5 weeks after stroke, which indicates that the reorganized white matter may be functional. These functional microvessels and neuronal fibers rebuild the microstructure and increase the cerebral tissue density along the ischemic boundary. Thus, the reparative cerebral tissue may resist the ventricular expansion and cerebral shrinkage. In control animals, non-enhanced angiogenesis was present 4 ~ 5 weeks after stroke as shown by T_2* map or SWI (Fig. 5 g, h). No apparent elevation of CBF and reorganization of neuronal fibers were detected at 6 weeks after stroke by CBF and DA maps in the present MRI study, compared with EPO treated animals. Therefore, the ischemic cerebral tissue in the control rats may not be able to resist the ipsilateral ventricular

expansion and tissue shrinkage. As a result, the reparative dense cerebral tissue in EPO treated rats significantly reduced the expansion rate of the ipsilateral ventricle starting from 4 weeks after stroke, compared with control rats (Fig. 4 a). Moreover, the reparative cerebral tissue of treated rats also stopped further atrophy of the ipsilateral hemisphere starting 4 weeks post stroke, 1 week earlier than in the control group (Fig. 4 b). At 6 weeks after stroke, cerebral tissue volume (excluding ventricle from hemisphere) ratio (ipsilateral vs contralateral) was significantly different ($p < 0.02$) with 89.8% in the treated group, contrast to 83.9% in the control group (Fig. 4 c). Thus, our results indicate that delayed EPO treatment of stroke repaired cerebral tissue and reduced ipsilateral brain atrophy.

Cerebral atrophy is a common feature of many diseases that affect the brain. With a discrete unilateral brain traumatic injury model in the mouse, global reduction in brain matter and bilateral enlargement of ventricles were observed at both 3 and 9 months after traumatic parietal lesion, and early EPO treatment beginning immediately after lesioning for 14 days prevented brain atrophy measured at 9 months (Siren et al, 2006). In an experimental stroke model in the mouse, where the unilateral MCA was cauterized, a mild protective effect with respect to brain atrophy was observed in ipsilateral hemisphere at 35 days post stroke with EPO administration subcutaneously at 24, 48 and 72 hours after the onset of stroke at a dose of 1,000 μg/kg (Taguchi et al, 2007). In the clinic, most stroke patients show cerebral atrophy in the chronic stage of stroke (Walters et al, 2003; Kraemer et al, 2004). To our knowledge, few systematic experimental studies addressing brain repair against atrophy after stroke have been performed. Improved knowledge of cerebral repair after stroke may provide a new target for intervention. In the present study, an embolic stroke model of rat was employed and brain atrophy in the ipsilateral hemisphere was observed at 6 weeks after ischemia. The ipsilateral ventricle enlarges and the hemisphere shrinks because of brain tissue cavitation (Dereski et al, 1993; Wei et al, 2006). However, the volume of cerebral tissue in the ipsilateral hemisphere is significantly greater in the EPO treated group than in the control group. EPO treatment significantly reduced the ipsilateral atrophy by decreasing ventricular expansion and hemispheric shrinkage starting from 5 weeks after stroke.

EPO treatment of embolic stroke may be either neuroprotective or neurorestorative depending upon when it is administered. Administration of EPO within a few hours after stroke is neuroprotective and significantly reduces infarct volume (Brines et al, 2000; Sirén et al, 2001; Leist et al, 2004; Wang et al, 2007). As a neuroprotective agent, EPO represses apoptosis by upregulating Bcl-xL, an anti-apoptotic gene of the Bcl-2 family (Silva et al, 1996; Wagner et al, 2000). In addition to this anti-apoptotic effect, EPO has anti-inflammatory effects which derive from its inhibition of tumor necrosis factor, a specific pro-inflammatory cytokine, by reducing activation of astrocytes as well as influx of inflammatory microglia into the ischemic region (Viviani et al, 1995; Villa et al, 2003). Both anti-apoptotic and anti-inflammatory effects have been proposed as likely mechanisms contributing to the neuroprotective action of EPO (Sirén et al, 2001).

A recent report on the Phase III clinical trial for the treatment of acute ischemic stroke with EPO demonstrated increased mortality and hemorrhage in EPO treated patients compared with control (Ehrenreich et al, 2009). The apparent adverse effects of the EPO treatment stand in contrast to the robust preclinical data indicating a therapeutic benefit of EPO treatment. However, careful review of the trial shows that 63% of patients enrolled in this trial also received tPA, and that many of these patients were treated at or beyond the therapeutic window for tPA. Data from the clinical trial also indicate that it was these patients that drove the adverse response to EPO. Thus, this clinical study might not bias the development of EPO as a restorative monotherapy.

In summary, treatment of embolic stroke with EPO in rats initiated from 24 hours and daily for 7 days augmented angiogenesis, neurogenesis and white matter reorganization, which resulted in cerebral tissue repair after stroke and subsequently led to a significantly reduced expansion of the ipsilateral ventricle and shrinkage of the ipsilateral hemisphere, protecting brain from further atrophy. The results of this study suggest that delayed EPO treatment restructures cerebral tissue damaged after stroke to resist the ventricular expansion and cerebral shrinkage.

Acknowledgments

This work was supported by NINDS grants PO1 NS23393, PO1 NS42345, RO1 NS43324, RO1 NS48349, HL64766 and the Mort and Brigitte Harris Foundation.

References

Adams HP, Adams RJ, Brott T, del Zoppo GJ, Furlan A, Goldstein LB, Grubb RL, Higashida R, Kidwell C, Kwiatkowski TG, Marler JR, Hademenos GJ. Guidelines for the early management of patients with ischemic stroke. Stroke. 2003; 34:1056–1083. [PubMed: 12677087]

Adams HP, Adams RJ, del Zoppo GJ, Goldstein LB. Guidelines for the Early Management of Patients with Ischemic Stroke. Stroke. 2005; 36:916–921. [PubMed: 15800252]

Arvidsson A, Collin T, Kirik D, Kokaia Z, Lindvall O. Neuronal replacement from endogenous precursors in the adult brain after stroke. Nat Med. 2002; 8:963–970. [PubMed: 12161747]

Brines ML, Ghezzi P, Keenan S, Agnello D, de Lanerolle NC, Cerami C, Itri LM, Cerami A. Erythropoietin crosses the blood-brain barrier to protect against experimental brain injury. Proc Natl Acad Sci USA. 2000; 97:10526–10531. [PubMed: 10984541]

Cramer SC, Chopp M. Recovery recapitulates ontogeny. Trends Neurosci. 2000; 23:265–271. [PubMed: 10838596]

Dereski MO, Chopp M, Knight RA, Rodolosi LC, Garcia JH. The heterogeneous temporal evolution of focal ischemic neuronal damage in the rat. Acta Neuropathol. 1993; 85:327–333. [PubMed: 8460534]

Ding G, Jiang Q, Zhang L, Zhang ZG, Knight R, Soltanian-Zadeh H, Lu M, Ewing J, Li Q, Whitton PA, Chopp M. Multiparametric ISODATA analysis of embolic stroke and rt-PA intervention in rat. J Neurol Sci. 2004; 223:135–143. [PubMed: 15337614]

Ding G, Jiang Q, Li L, Zhang L, Zhang ZG, Ledbetter KA, Gollapalli L, Panda S, Li Q, Ewing JR, Chopp M. Angiogenesis Detected After Embolic Stroke in Rat Brain Using Magnetic Resonance T2*WI. Stroke. 2008a; 39:1563–1568. [PubMed: 18356548]

Ding G, Jiang Q, Li L, Zhang L, Zhang ZG, Ledbetter KA, Panda S, Davarani SPN, Athiraman H, Li Q, Ewing JR, Chopp M. Magnetic resonance imaging investigation of axonal remodeling and angiogenesis after embolic stroke in sildenafil-treated rats. J Cereb Blood Flow & Metab. 2008b; 28:1440–1448. [PubMed: 18418368]

Ehrenreich H, Weissenborn K, Prange H, Schneider D, Weimar C, Wartenberg K, Schellinger PD, Bohn M, Becker H, Wegrzyn M, Jaehnig P, Herrmann M, Knauth M, Baehr M, Heide W, Wagner A, Schwab S, Reichmann H, Schwendemann G, Dengler R, Kastrup A, Bartels C. Recombinant human erythropoietin in the treatment of acute ischemic stroke. Stroke. 2009; 40:e647–e656. [PubMed: 19834012]

Ghezzi P, Brines M. Erythropoietin as an antiapoptotic, tissue-protective cytokine. Cell Death Differentiation. 2004; 11:S37–S44.

Grotta JC, Burgin WS, El-Mitwalli A, Long M, Campbell M, Morgenstern LB, Malkoff M, Alexanderov AV. Intravenous tissue-type plasminogen activator therapy for ischemic stroke: Houston experience 1996 to 2000. Arch Neurol. 2001; 58:2009–2013. [PubMed: 11735774]

Haacke ME, Xu Y, Cheng YC, Reichenbach JR. Susceptibility weighted imaging (SWI). Magn Reson Med. 2004; 52:612–618. [PubMed: 15334582]

Hoehn-Berlage M, Eis M, Back T, Kohno K, Yamashita K. Changes of Relaxation Times (T1, T2) and Apparent Diffusion Coefficient After Permanent Middle Cerebral Artery Occlusion in the Rat:

Temporal Evolution, Regional Extent, and Comparison with Histology. Magn Reson Med. 1995; 34:824–834. [PubMed: 8598809]

Jacobs MA, Windham JP, Soltanian-Zadeh H, Peck DJ, Knight RA. Registration and warping of magnetic resonance images to histological sections. Med Phys. 1999; 26:1568–1578. [PubMed: 10501057]

Jelkmann W, Hellwig-Burgel T. Biology of erythropoietin. Adv Exp Med Biol. 2001; 502:169–187. [PubMed: 11950137]

Kraemer M, Schormann T, Hagemann G, Qi B, Witte OW, Seitz RJ. Delayed shrinkage of the brain after ischemic stroke: preliminary observations with voxel-guided morphometry. J Neuroimaging. 2004; 14:265–272. [PubMed: 15228769]

Krupinski J, Kaluza J, Kumar P, Kumar S, Wang JM. Role of angiogenesis in patients with cerebral ischemic stroke. Stroke. 1994; 25:1794–8179. [PubMed: 7521076]

Leist M, Ghezzi P, Grasso G, Bianchi R, Villa P, Fratelli M, Savino C, Bianchi M, Nielsen J, Gerwien J, Kallunki P, Larsen AK, Helboe L, Christensen S, Pedersen LO, Nielsen M, Torup L, Sager T, Sfacteria A, Erbayraktar S, Erbayraktar Z, Gokmen N, Yilmaz O, Cerami-Hand C, Xie QW, Coleman T, Cerami A, Brines M. Derivatives of erythropoietin that are tissue protective but not erythropoietic. Science. 2004; 305:239–242. [PubMed: 15247477]

Li L, Jiang Q, Zhang L, Ding G, Zhang ZG, Li Q, Ewing JR, Lu M, Panda S, Ledbetter KA, Whitton PA, Chopp M. Angiogenesis and improved cerebral blood flow in the ischemic boundary area detected by MRI after administration of sildenafil to rats with embolic stroke. Brain Res. 2007; 1132:185–192. [PubMed: 17188664]

Li L, Jiang Q, Ding G, Zhang L, Zhang ZG, Li Q, Panda S, Kapke A, Lu M, Ewing JR, Chopp M. MRI identification of white matter reorganization enhanced by erythropoietin treatment in a rat model of focal ischemia. Stroke. 2009; 40:936–941. [PubMed: 19150870]

Morgenstern LB, Staub L, Chan W, Wein TH, Bartholomew LK, King M, Felberg RA, Burgin WS, Groff J, Hickenbottom SL, Saldin K, Demchuk AM, Kalra A, Dhingra A, Grotta JC. Improving delivery of acute stroke therapy: The TLL Temple Foundation Stroke Project. Stroke. 2002; 33:160–166. [PubMed: 11779906]

Ohab JJ, Fleming S, Blesch A, Carmichael ST. A neurovascular niche for neurogenesis after stroke. J Neurosci. 2006; 26:13007–13016. [PubMed: 17167090]

Ovbiagele B, Kidwell CS, Starkman S, Saver JL. Neuroprotective agents for the treatment of acute ischemic stroke. Curr Neurol Neurosci Rep. 2003; 3:9–20. [PubMed: 12507405]

Parent JM, Vexler ZS, Gong C, Derugin N, Ferriero DM. Rat forebrain neurogenesis and striatal neuron replacement after focal stroke. Ann Neurol. 2002; 52:802–813. [PubMed: 12447935]

Parent JM, Silverstein FS. Replacing neocortical neurons after stroke. Ann Neurol. 2007; 61:185–186. [PubMed: 17387724]

Peck DJ, Spickler EM, Knight RA, Hearshen DO, Windham JP. Analysis of the evolution of focal cerebral ischemia in the rat using the eigenimage filter. Magn Reson Med. 1992; 26:259–273. [PubMed: 1513250]

Plane JM, Whitney JT, Schallert T, Parent JM. Retinoic acid and environmental enrichment alter subventricular zone and striatal neurogenesis after stroke. Exp Neurol. 2008; 214:125–134. [PubMed: 18778705]

Plate KH, Beck H, Danner S, Allegrini PR, Wiessner C. Cell type specific upregulation of vascular endothelial growth factor in an MCA-occlusion model of cerebral infarct. J Neuropathol Exp Neurol. 1999; 58:654–666. [PubMed: 10374756]

Silva M, Grillot D, Benito A, Richard C, Nunez G, Fernandez-Luna JL. Erythropoietin can promote erythroid progenitor survival by repressing apoptosis through Bcl-XL and Bcl-2. Blood. 1996; 88:1576–1582. [PubMed: 8781412]

Sirén AL, Fratelli M, Brines M, Goemans C, Casagrande S, Lewczuk P, Keenan S, Gleiter C, Pasquali C, Capobianco A, Mennini T, Heumann R, Cerami A, Ehrenreich H, Ghezzi P. Erythropoietin prevents neuronal apoptosis after cerebral ischemia and metabolic stress. Proc Natl Acad Sci USA. 2001; 98:4044–4049. [PubMed: 11259643]

Sirén AL, Radyushkin K, Boretius S, Kaemmer D, Riechers CC, Natt O, Sargin D, Watanabe T, Sperling S, Michaelis T, Price J, Meyer B, Frahm J, Ehrenreich H. Global brain atrophy after

unilateral parietal lesion and its prevention by erythropoietin. Brain. 2006; 129:480–489. [PubMed: 16339796]

Taguchi A, Wen Z, Myojin K, Yoshihara T, Nakagomi T, Nakayama D, Tanaka H, Soma T, Stern DM, Naritomi H, Matsuyama T. Granulocyte colony-stimulating factor has a negative effect on stroke outcome in a murine model. Eur J Neuros. 2007; 26:126–133.

Teng H, Zhang ZG, Wang L, Zhang RL, Zhang L, Morris D, Gregg SR, Wu Z, Jiang A, Lu M, Zlokovic BV, Chopp M. Coupling of angiogenesis and neurogenesis in cultured endothelial cells and neural progenitor cells after stroke. J Cereb Blood Flow Metab. 2008; 28:764–771. [PubMed: 17971789]

van Gelderen P, de Vleeschouwer MHM, DesPres D, Pekar J, van Zijl PCM, Moonen CTW. Water diffusion and acute stroke. Magn Reson Med. 1994; 31:154–163. [PubMed: 8133751]

Villa P, Bigini P, Mennini T, Agnello D, Laragione T, Cagnotto A, Viviani B, Marinovich M, Cerami A, Coleman TR, Brines M, Ghezzi P. Erythropoietin selectively attenuates cytokine production and inflammation in cerebral ischemia by targeting neuronal apoptosis. J Exp Med. 2003; 198:971–975. [PubMed: 12975460]

Viviani B, Rossi AD, Chow SC, Nicotera P. Organotin compounds induce calcium overload and apoptosis in PC12 cells. Neurotoxicology. 1995; 16:19–25. [PubMed: 7603641]

Wagner KU, Claudio E, Rucker EB III, Riedlinger G, Broussard C, Schwartzberg PL, Siebenlist U, Hennighausen L. Conditional deletion of the Bcl-x gene from erythroid cells results in hemolytic anemia and profound splenomegaly. Development. 2000; 127:4949–4958. [PubMed: 11044408]

Wakefield AJ, More LJ, Difford J, McLaughlin JE. Immunohistochemical study of vascular injury in acute multiple sclerosis. J Clin Pathol. 1994; 47:129–133. [PubMed: 8132826]

Walters RJL, Fox NC, Schott JM, Crum WR, Stevens JM, Rossor MN, Thomas DJ. Transient ischaemic attacks are associated with increased rates of global cerebral atrophy. J Neurol Neurosurg Psychiatry. 2003; 74:213–216. [PubMed: 12531953]

Wang L, Zhang ZG, Wang Y, Zhang RL, Chopp M. Treatment of stroke with erythropoietin enhances neurogenesis and angiogenesis and improves neurological function in rats. Stroke. 2004; 35:1732–1737. [PubMed: 15178821]

Wang Y, Zhang ZG, Rhodes K, Renzi M, Zhang RL, Kapke A, Lu M, Pool C, Heavner G, Chopp M. Post-ischemic treatment with erythropoietin or carbamylated erythropoietin reduces infarction and improves neurological outcome in a rat model of focal cerebral ischemia. Brit J Pharm. 2007; 151:1377–1384.

Wei L, Han BH, Li Y, Keogh CL, Holtzman DM, Yu SP. Cell death mechanism and protective effect of erythropoietin after focal ischemia in the whisker-barrel cortex of neonatal rats. J Pharmacol Exp Ther. 2006; 317:109–116. [PubMed: 16357210]

Williams DS, Detre JA, Leigh JS, Koretsky AP. Magnetic resonance imaging of perfusion using spin inversion of artery water. Proc Natl Acad Sci USA. 1992; 89:212–216. [PubMed: 1729691]

Yu SW, Friedman B, Cheng Q, Lyden PD. Stroke-evoked angiogenesis results in a transient population of microvessels. J Cereb Blood Flow Metab. 2007; 27:755–763. [PubMed: 16883352]

Zhang RL, Chopp M, Zhang ZG, Jiang Q, Ewing JR. A rat model of focal embolic cerebral ischemia. Brain Res. 1997; 766:83–92. [PubMed: 9359590]

Zhang RL, Zhang ZG, Zhang L, Chopp M. Proliferation and differentiation of progenitor cells in the cortex and the subventricular zone in the adult rat after focal cerebral ischemia. Neuroscience. 2001; 105:33–41. [PubMed: 11483298]

Zhang RL, Zhang Z, Wang L, Wang Y, Gousev A, Zhang L, Ho KL, Morshead C, Chopp M. Activated neural stem cells contribute to stroke-induced neurogenesis and neuroblast migration toward the infarct boundary in adult rats. J Cereb Blood Flow Metab. 2004; 24:441–448. [PubMed: 15087713]

Zhang RL, Zhang ZG, Chopp M. Neurogenesis in the adult ischemic brain: generation, migration, survival, and restorative therapy. Neuroscientist. 2005; 11:408–416. [PubMed: 16151043]

Zhang ZG, Zhang L, Jiang Q, Zhang R, Davies K, Powers C, Bruggen N, Chopp M. VEGF enhances angiogenesis and promotes blood-brain barrier leakage in the ischemic brain. J Clin Invest. 2000; 106:829–838. [PubMed: 11018070]

Zhang ZG, Chopp M. Neurorestorative therapies for stroke: underlying mechanisms and translation to the clinic. Lancet Neurol. 2009; 8:491–500. [PubMed: 19375666]

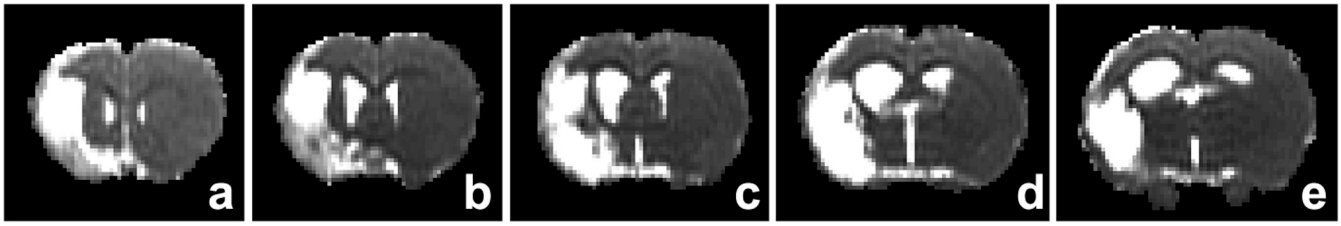

Figure 1.
T_2 maps of central five slices in order (a–e) were used to measure total volumes of the ipsilateral and contralateral ventricles and hemispheres.

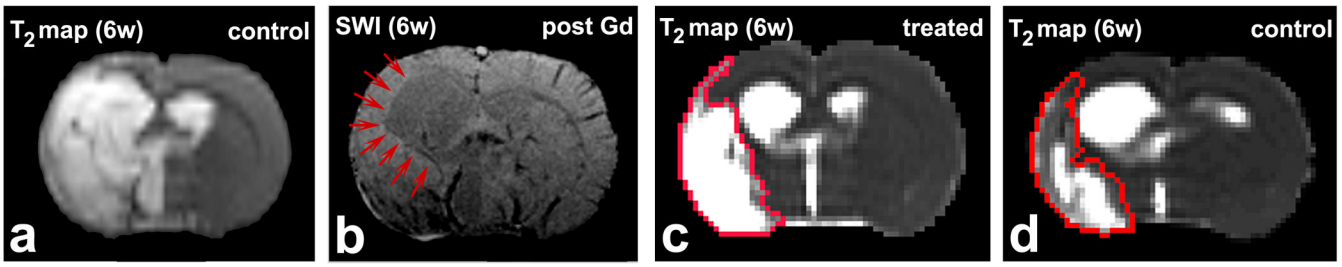

Figure 2.

A typical case, where the ischemic lesion areas can not distinguished from ventricle in T_2 maps (a). An SWI image (b) was used to demarcate the edge of the ventricle, as indicated by red arrows. T_2 maps at 6 weeks after stroke from a representative EPO-treated rat (c) and a control rat (d) demonstrated that the ipsilateral ventricle expansion was reduced in the treated rat relative to the control one, lesion areas indicated by red borders were identified by T_2 values.

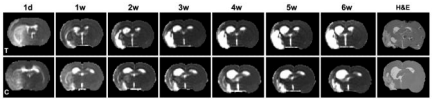

Figure 3.

Serial T2WI images of an EPO treated rat (upper row) exhibited gradual expansion of the ipsilateral ventricle starting 1 to 6 weeks after stroke compared to the contralateral ventricle. The ipsilateral ventricle in the controls (lower row) exhibited both faster and greater expansion compared to the treated rats. The H&E sections (last column) histologically confirmed the MRI findings. The ipsilateral ventricle was smaller than the contralateral ventricle at 24 hours due to ischemic edema (first column).

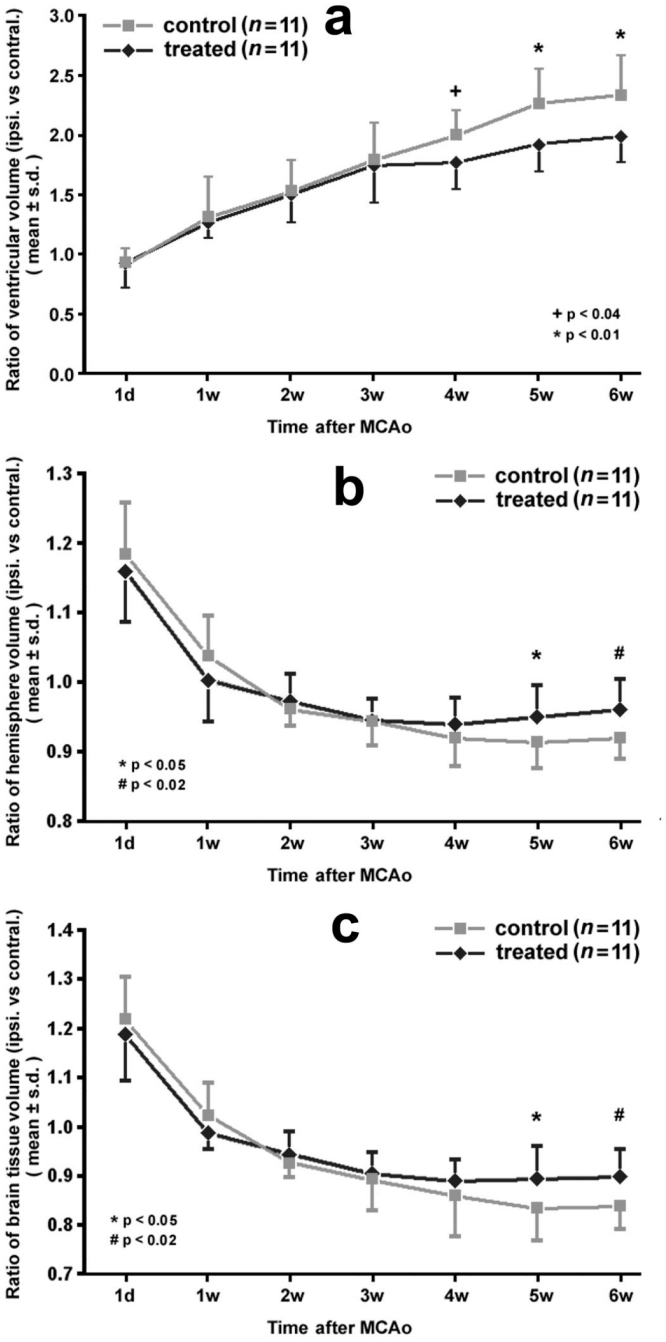

Figure 4.

Ventricular volume ratios (ipsilateral *vs* contralateral) of both treated and control groups increased monotonically from 1 day to 6 weeks after stroke (a). The mean ratios were significantly lower for the treated rats than controls starting 4 weeks after stroke. The hemispheric volume ratio (ipsilateral *vs* contralateral) was significantly different between groups starting 5 weeks after stroke (b). Excluding the ventricle, changes of parenchymal volume ratio (c) were similar to the hemispheric ratio. Cerebral tissue loss in the EPO treated rats was significantly reduced from 5 weeks after stroke compared to the controls.

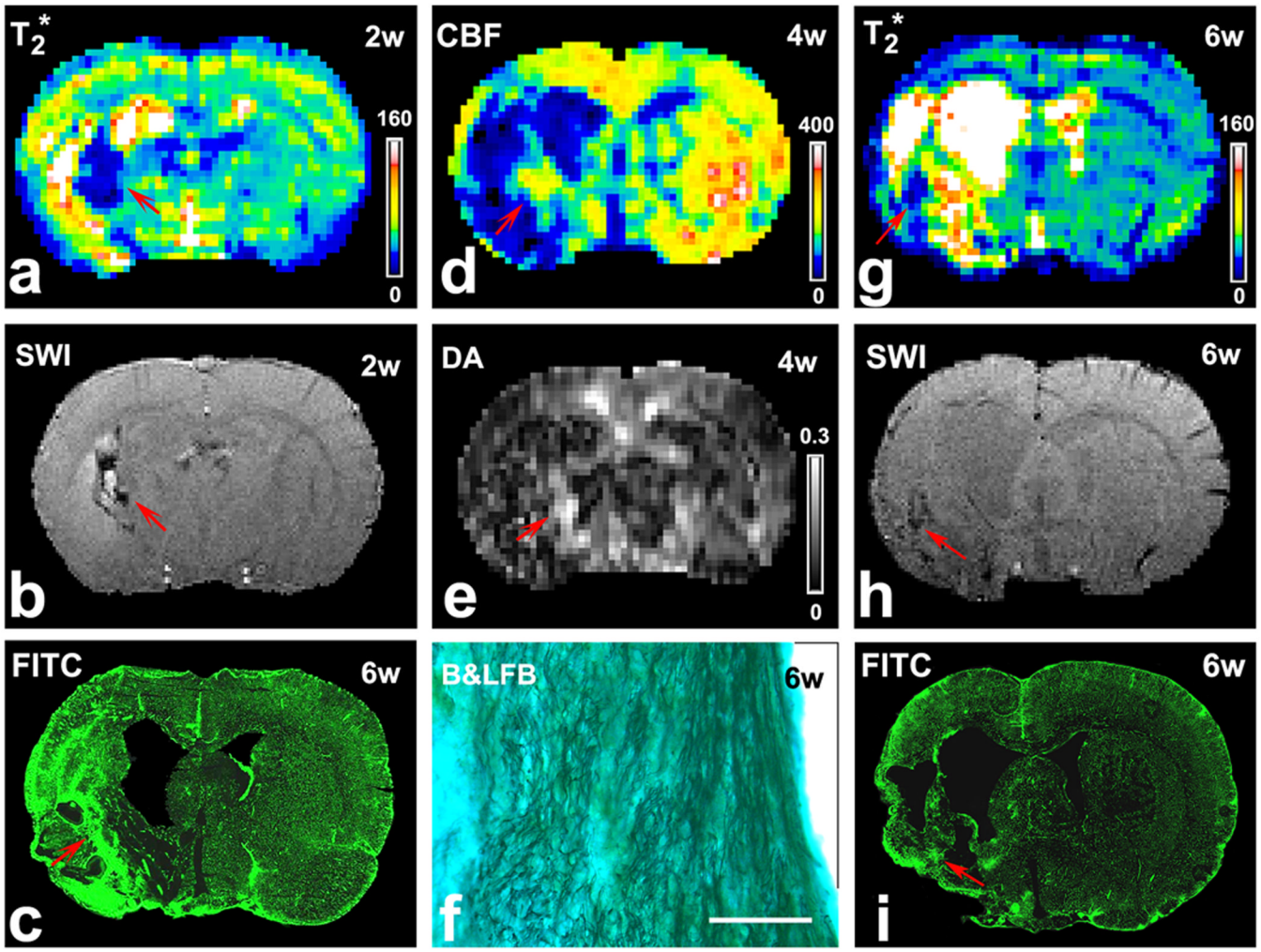

Figure 5.

Images of T_2* map (a) or SWI (b) at 2 weeks after stroke demonstrated angiogenesis (red arrows) in a representative EPO treated rat. FITC-dextran stained sections (c) showed increased microvessels in this region (red arrow). Elevated CBF was found in the same area (red arrow) at 4 weeks after stroke (d). Increased DA values (e, red arrow) were located in the same area as in the T_2* map (a), SWI (b) and CBF (d). B&LFB stained sections demonstrated increased numbers of axons and highly ordered neuronal fibers in this region (f, bar = 100μm). In a representative control rat, T_2* map (g) or SWI (h) at 6 weeks after stroke demonstrated smaller area where angiogenesis might happen (red arrows), which was confirmed by FITC-dextran stained sections (i, red arrow).

Table 1

Volumes (mm^3) of contralateral ventricle and hemisphere measured by T_2 maps using five central slices

	Ventricle		hemisphere	
	EPO (n=11)	**saline (n=11)**	**EPO (n=11)**	**saline (n=11)**
1d	15.2±4.6	16.5±3.7	259.9±26.0	265.0±21.2
1w	14.3±3.8	16.5±3.9	290.9±10.2	286.4±16.3
2w	14.7±4.6	18.6±2.8	288.4±14.1	291.5±11.5
3w	16.4±3.9	19.3±3.5	289.4±12.2	291.6±14.7
4w	17.1±3.9	19.6±2.4	290.6±11.4	291.4±13.5
5w	15.8±4.2	18.4±3.7	290.2±11.9	288.6±15.4
6w	16.3±3.5	19.4±4.9	289.6±21.3	288.4±12.2

Note: no statistical differences were observed between EPO and saline groups in volumes of contralateral ventricle and hemisphere (significance was set as $p < 0.05$).